



Heterogeneous sulfate aerosol formation mechanisms during wintertime Chinese haze events: Air quality model assessment using observations of sulfate oxygen isotopes in Beijing

Jingyuan Shao^{1,2}, Qianjie Chen^{2,3}, Yuxuan Wang⁴, Xiao Lu¹, Pengzhen He⁵, Yele Sun⁶, Viral Shah^{2,7},
5 Randall V. Martin⁸, Sajeev Philip⁹, Shaojie Song⁷, Yue Zhao¹⁰, Zhouqing Xie⁵, Lin Zhang¹, and Becky
Alexander²

¹Laboratory for Climate and Ocean-Atmosphere Studies, Department of Atmospheric and Oceanic Sciences, School of Physics, Peking University, Beijing 100871, China

²Department of Atmospheric Sciences, University of Washington, Seattle, WA 98195, USA

10 ³Department of Chemistry, University of Michigan, MI 48109, USA

⁴Department of Earth and Atmospheric Sciences, University of Houston, Houston, TX 77204, USA

⁵Anhui Province Key Laboratory of Polar Environment and Global Change, School of Earth and Space Sciences, University of Science and Technology of China, Hefei, Anhui 230026, China

15 ⁶State Key Laboratory of Atmospheric Boundary Physics and Atmospheric Chemistry, Institute of Atmospheric Physics, Chinese Academy of Sciences, Beijing 100029, China

⁷School of Engineering and Applied Sciences, Harvard University, Cambridge, MA 02138, USA

⁸Department of Physics and Atmospheric Science, Dalhousie University, Halifax, Nova Scotia, Canada

⁹NASA postdoctoral program, NASA Ames Research Center, Moffett Field, CA, USA

20 ¹⁰School of Environmental Science and Engineering, Shanghai Jiao Tong University, Shanghai 200240, China

Correspondence to: Becky Alexander (beckya@uw.edu), Lin Zhang (zhanglg@pku.edu.cn) and Zhouqing Xie (zqxie@ustc.edu.cn)



25 Abstract

Air quality models have not been able to reproduce the magnitude of the observed concentrations of fine particulate matter (PM_{2.5}) during wintertime Chinese haze events. The discrepancy has been at least partly attributed to low biases in modeled sulfate production rates due to the lack of heterogeneous sulfate production on aerosols in the models. In this study, we explicitly implement four heterogeneous sulfate formation mechanisms into a regional chemical transport model, in addition to gas-phase and in-cloud sulfate production. We compare the model results with observations of sulfate concentrations and oxygen isotopes ($\Delta^{17}\text{O}(\text{SO}_4^{2-})$) in the winter of 2014-2015, the latter of which is highly sensitive to the relative importance of different sulfate production mechanisms. Model results suggest that heterogeneous sulfate production on aerosols accounts for about 20% of sulfate production in clean and polluted conditions, partially reducing the modeled low bias in sulfate concentrations. Model sensitivity studies in comparison with the $\Delta^{17}\text{O}(\text{SO}_4^{2-})$ observations suggest that heterogeneous sulfate formation is dominated by transition metal ion catalyzed oxidation of SO₂.

35

1. Introduction

China has experienced rapid urbanization and industrialization in recent years, which has led to significant growth in concentration of PM_{2.5} (particulate matter with aerodynamic diameter less than 2.5 μm) in Chinese megacities, particularly in Beijing (the capital of China) and surrounding areas (Zhang et al., 2016; Wang et al., 2014; Zhang et al., 2015). Extensive studies consistently show high PM_{2.5} levels in winter due to increased coal combustion for heating and a stable atmospheric boundary layer (Sun, et al., 2016; Sun, et al., 2014; Liu et al., 2015). The frequency and concentration of PM_{2.5} pollution negatively impacts human health and atmospheric visibility and results in economic losses (Gao et al., 2015; Lelieveld, et al., 2015; Zhang et al., 2015). The Chinese government has implemented a series of policies to improve air quality, and as a result the annual average PM_{2.5} concentration in Beijing decreased by ~20% from 2013 to 2017 (Sun et al., 2016; Zheng et al., 2018; Beijing Environment Protection Agency, 2018; Chinese State Council, 2013). Despite these improvements, PM_{2.5} concentrations in Beijing still regularly exceed the Chinese National Ambient Air Quality Standard (CNAAQs, 35 μg m⁻³ annual average) (Sun et al., 2016; Zhang et al., 2016; Beijing Environment Protection Agency, 2018).

50

Sulfate is one of the most important components of PM_{2.5}, representing 10-30% of PM_{2.5} mass in eastern China (Huang et al., 2014; Zhang et al., 2013; Wang et al., 2014; Sun et al., 2016; Shi et al., 2017). Recent observations show that the sulfate mass fraction of PM_{2.5} increases during haze pollution periods, indicating that sulfate is a key driver for severe haze events (Wang et al., 2014; Wang et al., 2016; Cheng et al., 2016; Li et al., 2017). Globally, sulfate production is dominated by the gas-phase oxidation of SO₂ by OH and aqueous-phase oxidation of S(IV) ($=\text{SO}_2 \cdot \text{H}_2\text{O} + \text{HSO}_3^- + \text{SO}_3^{2-}$) by H₂O₂, O₃, and O₂ catalyzed by transition metal ions (TMI) in cloud droplets (Stockwell and calvert, 1983; Schwartz, 1987; Harris

55



60 et al., 2013; Alexander et al., 2012; Chen et al., 2018). Heterogeneous sulfate production, which refers to aqueous-phase oxidation of S(IV) ($=\text{SO}_2 \cdot \text{H}_2\text{O} + \text{HSO}_3^- + \text{SO}_3^{2-}$) on the surface of and/or within the bulk pre-existing aerosols, is generally thought to be minor due to the low liquid water content of aerosols ($< 10^{-9} \text{ cm}^3 \text{ cm}^{-3}$) compared to clouds (10^{-8} to $10^{-6} \text{ cm}^3 \text{ cm}^{-3}$) (Jacob, 2000). However, recent studies have shown that traditional gas- and aqueous-phase chemistry in cloud droplets cannot explain rapid sulfate production observed during haze, suggesting missing sulfate formation mechanisms on aerosols in the models (Zheng et al., 2015; Chen et al., 2016; Zhang et al., 2015; Wang et al., 2014; Cheng et al., 2016; Huang et al., 2014). These missing sulfate formation mechanisms on aerosols include heterogeneous oxidation of SO_2 by
65 NO_2 (Cheng et al., 2016; Wang et al., 2016; Wang et al., 2018; Gao et al., 2016; Zhang et al., 2015) and O_2 catalyzed by TMI (Li et al., 2017a; Li et al., 2011) and via a free radical chain mechanism (Huie and Neta, 1984; Hung and Hoffman, 2015). The importance of these heterogeneous reactions remains highly uncertain due in part to uncertainties regarding the aerosol liquid water content, pH, and ionic strength, all of which impact heterogeneous reaction rates (Herrmann et al., 2015; Cheng et al., 2016). In particular, ambient aerosol pH cannot be directly measured, and thus represents a large source
70 of uncertainty (Hennigan et al., 2015).

Previous studies have calculated a large range of aerosol pH values (3.4 – 7.8) in Beijing using a thermodynamic model (ISORROPIA-II) (Fountoukis and Nenes, 2007). He et al. (2018) noted that the large differences in calculated aerosol pH depended on whether they assume aerosols exist in stable (Wang et al., 2016; He et al., 2018) or metastable state (Liu et al.,
75 2017; Guo et al., 2017; He et al., 2018). Stable-state assumption allows for the simultaneous existence of solid and aqueous phases, while the metastable-state assumption allows for the existence of aqueous phase only by assuming salts to be supersaturated in aerosols (Fountoukis and Nenes, 2007). Aerosol pH values simulated assuming stable state are near neutral (pH of 7), much higher than when assuming metastable state (pH of 4-5) during haze events in China (Guo et al., 2017; Liu et al., 2017; He et al., 2018). However, a recent study calculated aerosol pH of around 4.6 during Chinese haze
80 events for both the stable and metastable assumptions in ISORROPIA-II after fixing coding errors that impacted the stable state assumption (Song et al., 2018a). This casts doubt on the existence of neutral aerosol pH during Chinese haze events and thus the importance of the NO_2 oxidation pathway, which is not important under acidic conditions. Other factors, such as underestimate of NH_3 emissions (Zhang et al., 2017) and Ca^{2+} concentrations in aerosols (Shen et al., 2016) and the lack of consideration of organic acids in aerosol pH calculations (Wang et al., 2018), add additional uncertainties in estimates of
85 aerosol pH and thus sulfate production rates and mechanisms in Chinese haze events.

The oxygen isotopic composition $\Delta^{17}\text{O}$ ($\approx \delta^{17}\text{O} - 0.52 \times \delta^{18}\text{O}$) of secondary sulfate ($\Delta^{17}\text{O}(\text{SO}_4^{2-})$) reflects the relative importance of different oxidation mechanisms in sulfate production because some of the oxidants transfer unique oxygen isotope signatures to the sulfate oxidation product (Savarino et al., 2000). Sulfate production via S(IV) oxidation by O_3 and
90 H_2O_2 leads to positive $\Delta^{17}\text{O}(\text{SO}_4^{2-})$ values of 9.8‰ and 0.7‰, respectively, while all other oxidants lead to $\Delta^{17}\text{O}(\text{SO}_4^{2-})$ at or near 0‰ (Table S1) (Vicars and Savarino, 2014; Savarino and Thiemens, 1999; Lee and Schwartz, 1983; Holt et al.,



1981; Dubey et al., 1997). Primary sulfate, both natural (dust and sea salt) and anthropogenic (coal and oil combustion), also has $\Delta^{17}\text{O}(\text{SO}_4^{2-})$ values equal to 0‰ (Dominguez et al., 2008; Lee et al., 2001). Once formed, sulfate in the atmosphere does not undergo further isotope exchange. Surface observations around the world show that $\Delta^{17}\text{O}(\text{SO}_4^{2-})$ ranges from 0 to 6‰ (Alexander et al., 2012; Alexander et al., 2005; Chen et al., 2016; Dominguez et al., 2008; Jenkins and Bao, 2006; Lee et al., 2001; Lee and Thiemens, 2001; McCabe et al., 2006; Patris et al., 2007; He et al., 2018). Due to the large positive enrichment of sulfate formed from O_3 oxidation ($\Delta^{17}\text{O}(\text{SO}_4^{2-}) = 9.8$ ‰) and the strong pH dependence of this aqueous-phase reaction, $\Delta^{17}\text{O}(\text{SO}_4^{2-})$ is highly sensitive to pH.

In this work, we implement four heterogeneous reactions for sulfate formation (via H_2O_2 , O_3 , NO_2 , and TMI) into a global chemical transport model (GEOS-Chem) and compare the model results with observations of sulfate and SO_2 concentrations and $\Delta^{17}\text{O}(\text{SO}_4^{2-})$ in Beijing from October 2014 to January 2015. During this time period, Beijing held the Asia-Pacific Economic Cooperation (APEC) meeting from November 5-11, 2014. During and before APEC, strict emission control measures were applied in Beijing and its surrounding regions to improve air quality (Zhang et al., 2016). This paper is organized as follows. Section 2 describes the model simulations and the observations, and the method used to calculate heterogeneous sulfate production rates. Section 3 discusses model results with and without heterogeneous sulfate production considered in comparison with observed concentration and $\Delta^{17}\text{O}(\text{SO}_4^{2-})$. Section 4 discusses and explains the differences between our results and observations. Section 5 summarizes the main conclusions.

2 Methodology

2.1 GEOS-Chem model

We use the three-dimensional GEOS-Chem chemical transport model nested-grid version v10-01 (<http://www.geos-chem.org/>) to investigate sulfate formation mechanisms in Beijing, China between October 18, 2014 and January 17, 2015 (Wang et al., 2004; 2013; 2014; Zhang et al., 2015; 2016). The model has a horizontal resolution of $1/4^\circ$ latitude by $5/16^\circ$ longitude over East Asia ($70^\circ\text{E} - 140^\circ\text{E}$, $15^\circ\text{N} - 55^\circ\text{N}$) and 47 vertical levels up to 0.01 hPa (≈ 81 km). In the boundary layer where most heterogeneous sulfate production occurs, the vertical layer thickness is 120 - 150 m for the first 12 model layers (below 1700 m altitude). The model is driven by assimilated meteorological data from the NASA Goddard Earth Observing System (GEOS-FP), which has a temporal resolution of 3 hours (1 hour for surface quantities and mixing depths).

The model utilizes the global anthropogenic emission inventory EDGAR v4.2 (EC-JRC/PBL, <http://edgar.jrc.ec.europa.eu/>, 2011), overwritten by regional inventories such as the MIX Asian emission inventory over Asia (Li et al., 2017), EMEP over Europe (<http://www.emep.int/index.html>), and NEI2011 over the U.S. (<https://www.epa.gov/ttn/chief/net/2011inventory.html>). In particular, the MIX Asian emission inventory includes



25 emissions of SO₂, NO_x, CO, NH₃ and NMVOC at a spatial resolution of 0.25°×0.25° for the year 2010 (Li et al., 2017;
Geng et al., 2017). Mineral dust aerosols are emitted in the model as described in Fairlie et al. (2007) and distributed in
four size bins (radius of 0.1-1.0 μm, 1.0-1.8 μm, 1.8-3.0 μm, and 3.0-6.0 μm). In addition to natural dust, our model
includes anthropogenic dust (radius of 0.1 - 1.0 μm) released from anthropogenic activities such as
30 that anthropogenic dust accounts for about 25% of the PM_{2.5} mass fraction in Beijing (Zhang et al., 2015; Phillipet al.,
2017).

The sulfate-nitrate-ammonium aerosol system is fully coupled to oxidant chemistry (Park et al., 2004), with aerosol pH,
ionic strength, and aerosol water content (AWC) calculated from the ISORROPIA-II thermodynamic equilibrium model
35 (Fountoukis and Nenes, 2007) that was implemented into GEOS-Chem by Pye et al. (2009). In the standard model
(Run_Std), sulfate is produced from gas-phase oxidation of SO₂ by OH, aqueous-phase oxidation of S(IV) (=SO₂ · H₂O +
HSO₃⁻ + SO₃²⁻) by H₂O₂ and O₃ in cloud droplets, and heterogeneous oxidation on sea-salt aerosols by O₃ (Alexander et al.,
2005). Primary anthropogenic emissions of sulfate constitute 3.1% of total anthropogenic sulfur emissions in China and 1.5%
- 3.5% elsewhere. Sulfate is removed from the atmosphere via dry (Zhang et al., 2001) and wet (Liu et al., 2001) deposition,
40 with a global lifetime of about 4 days (Alexander et al., 2005).

We performed three simulations at high horizontal resolution (1/4°×5/16°) and seven sensitivity simulations at low
horizontal resolution (4°×5°) to investigate sulfate formation mechanisms in Beijing, as summarized in Table 1. In the
model simulation Run_TMI, we implemented the in-cloud TMI-catalyzed aqueous-phase S(IV) oxidation by O₂ chemistry
45 into the model following Alexander et al. (2009), but reduced the solubility of trace metals Fe and Mn derived from natural
dust (from 1% to 0.45% for Fe and from 50% to 5% for Mn) to better match observations (Desboeufs et al., 2001; 2005;
Chuang et al., 2005). In the model, Fe from natural dust ([Fe]_{nat}) is 3.5% of total dust mass and Mn from natural dust
([Mn]_{nat}) is a factor of 50 lower than [Fe]_{nat} (Alexander et al., 2009). Anthropogenic Mn ([Mn]_{ant}) and Fe ([Fe]_{ant}) are scaled
to the abundance of primary anthropogenic sulfate due to common sources and lifetimes. [Mn]_{ant} is 1/300 of primary sulfate
50 concentration and [Fe]_{ant} is 10 times that of [Mn]_{ant} as described in Alexander et al. (2009). Only soluble Fe and Mn in the
oxidation states Fe(III) and Mn(II) catalyze S(IV) oxidation. For Fe, we assume solubility of 10% for [Fe]_{ant} and 0.45% of
[Fe]_{nat} in cloud water, respectively, with 10% in the form of Fe(III) during daytime and 90% at night. For Mn, we assume a
solubility of 50% for [Mn]_{ant} and 5% for [Mn]_{nat} in cloud water, respectively, with 100% in the form of Mn(II). In addition,
we considered the impacts of acidity and ionic strength on TMI-catalyzed reaction rates following Cheng et al. (2016) as
55 described in the SI (Table S2), since the ionic strength of cloud liquid water can reach 0.01M during polluted periods
(Herrmann et al., 2015).

In the model run Run_Het, we added four heterogeneous sulfate production mechanisms (via H₂O₂, O₃, NO₂, and TMI) on



60 aerosols into the model, in addition to TMI-catalyzed oxidation in clouds. Implementation of these reactions in the model is described in Sect. 2.2. In Run_Het, heterogeneous sulfate production on aerosols only occurs when relative humidity (RH) is greater than 50%, effectively assuming that aerosol water content is too low for sufficient heterogeneous sulfate production at $RH < 50\%$. When $RH < 50\%$, aerosols are assumed to remain crystallized until reaching the deliquescence relative humidity (DRH). This is consistent with observations in previous studies showing that sulfate production rates in Chinese haze are positively correlated with RH (Sun et al., 2013; Zhang et al., 2015; Wang et al., 2016). Ca^{2+} and Mg^{2+} cations from dust (both natural and anthropogenic) are included in the aerosol thermodynamic calculations (aerosol pH, 65 aerosol water content, ionic strength). We assume that Ca^{2+} and Mg^{2+} cations constitute 3.0% and 0.6% of the dust by mass, respectively, based on observations near East Asian dust source regions (Fairlie et al., 2010). We performed seven sensitivity studies based on Run_Het but with prescribed values of aerosol pH to examine the dependence of model results on aerosol pH alone (Table 1).

70 For all model simulations, sulfate produced from each oxidation pathway is labeled as a separate “tracer” in the model with a corresponding $\Delta^{17}O(SO_4^{2-})$ values (9 sulfate tracers in total, Table S1) as originally described in Alexander et al. (2005). Primary anthropogenic sulfate is also included as a separate tracer in the model with $\Delta^{17}O = 0\text{‰}$ (Lee et al., 2002). The details for calculating $\Delta^{17}O(SO_4^{2-})$ in the model are described in the supplement (Text S1).

75

2.2 Heterogeneous sulfate production on aerosols

Heterogeneous S(IV) oxidation in the model occurs on all aerosol types, including sulfate-nitrate-ammonium, dust, black carbon, organic carbon, and sea-salt aerosols. The heterogeneous sulfate production rate on aerosol (P_{het}) is calculated in the model assuming a first-order loss of SO_2 or oxidant (depending on which is the rate limiting step) via uptake by the 80 aerosol (Eq. 1).

$$P_{het} = k[SO_2 \text{ or oxidant}] \quad (1)$$

The first-order loss rate constant (k , s^{-1}) is calculated using the reaction probability formulation in Jacob (2000) (Eq. 2).

85

$$k = \left(\frac{r_a}{D_g} + \frac{4}{v\gamma} \right)^{-1} A \quad (2)$$

where r_a is the radius of the specific type of aerosol (cm); A is the total aerosol surface area per unit volume of air for the specific type of aerosol ($cm^2 \text{ cm}^{-3}$); v is the mean molecular speed of SO_2 or the oxidant ($cm \text{ s}^{-1}$); D_g represents the gas-phase molecular diffusion coefficient of SO_2 or the oxidant ($cm^2 \text{ s}^{-1}$) calculated as:

$$90 \quad D_g = \frac{9.45110^{17} \times \sqrt{T \times (3.47 \times 10^{-2} + (1/M))}}{\rho_{air}} \quad (3)$$



where T is air temperature (K), ρ_{air} is air density (molecule m^{-3}), and M represents the molar mass of SO_2 or the oxidant (g mol^{-1}). The reaction probability (γ) is defined as the probability that a molecule impacting the aerosol surface undergoes a chemical reaction (Ravishankara, 1997; Jacob, 2000). Due to limited understanding of sulfate formation on aerosols, chemical transport models typically calculate heterogeneous sulfate production rate on aerosols by assuming the bulk first-order uptake of SO_2 and using a wide range of γ values (10^{-4} - 10^{-1}) (Wang et al., 2014; Zhang et al., 2014). However, the relative contribution of different sulfate production mechanisms, which is important to inform air pollution mitigation efforts, cannot be determined with this simplified approach.

In this study, we use a more specific approach to calculate γ for each heterogeneous sulfate production mechanisms following Jacob (2000) and Ammann et al. (2013) (Eq. 4).

$$\gamma = \left[\frac{1}{\alpha} + \frac{v}{4K^*RT\sqrt{D_a k_{chem}}} \cdot \frac{1}{f_r} \right]^{-1} \quad (4)$$

where α is the mass accommodation coefficient (unitless); k_{chem} is the pseudo first-order aqueous-phase chemical rate constant between S(IV) and the oxidant (O_3 , H_2O_2 , NO_2 or O_2) (s^{-1}) (Table S2); D_a is the aqueous-phase molecular diffusion coefficient of SO_2 or the oxidant ($\text{cm}^2 \text{s}^{-1}$); K^* is the effective Henry's law constant of SO_2 or the oxidant (M atm^{-1}); R is the universal gas constant ($\text{L atm mol}^{-1} \text{K}^{-1}$), and f_r is reacto-diffusive correction term that compares the radius of aerosols (r_a) with the reacto-diffusive length scale of the reaction (l):

$$f_r = \coth \frac{r_a}{l} - \frac{l}{r_a} \quad (5)$$

$$l = \sqrt{\frac{D_a}{k_{chem}}} \quad (6)$$

In the model, the heterogeneous sulfate production rate from the TMI-catalyzed reaction is calculated as first-order uptake in SO_2 . All other heterogeneous sulfate production pathways are calculated as first-order uptake in the oxidant (H_2O_2 , O_3 , and NO_2). This is based on whether the heterogeneous sulfate production on aerosol is limited by the availability of SO_2 or the oxidant. For example, for aerosol pH values less than 6, heterogeneous sulfate production rates calculated as a first-order loss in SO_2 or the oxidant are similar (Figure S1(b)). For aerosol pH values greater than 6, heterogeneous sulfate production rates calculated as a first-order loss in SO_2 are higher than those calculated as a first-order loss in the oxidants O_3 and NO_2 . The reaction rate for S(IV) oxidation by O_3 and NO_2 increases with increasing pH, and at high pH values γ is limited by the mass accommodation coefficient and becomes independent of pH. The mass accommodation coefficients for O_3 (2×10^{-3}) and NO_2 (2×10^{-4}) are much lower than for SO_2 (0.23). The mass accommodation coefficient for H_2O_2 (0.11) is



similar to SO₂, and γ for the reaction of S(IV) with H₂O₂ was limited by the oxidant concentration. More details on first-order loss rates are described in Text S2.

25 In addition to the model simulations described in Table 1, we have also examined heterogeneous oxidation of SO₂ by O₂ on the surface of acidic microdroplets (Hung and Hoffman, 2015) and by HOBr (Chen et al., 2016; 2017). The results are described in the supplementary material (Text S2).

2.3 Observations of sulfate concentrations and oxygen isotopic composition

30 Between 17 October 2014 and 20 January 2015, PM_{2.5} samples were collected every 12 hours for daytime (08:00-20:00 Beijing Time) and nighttime (20:00-08:00 Beijing Time) conditions at the campus of University of the Chinese Academy of Sciences (40.41°N, 116.68°E, 20 m from the ground) in Beijing, around 60 km northeast of downtown. The oxygen-17 excess of sulfate ($\Delta^{17}\text{O}(\text{SO}_4^{2-})$) on these PM_{2.5} samples were measured at University of Washington, Seattle. A detailed description of sampling and measurements of $\Delta^{17}\text{O}(\text{SO}_4^{2-})$ can be found in He et al. (2018). Observations of hourly sulfate
35 concentrations were conducted at the Institute of Atmospheric Physics (IAP), Chinese Academy of Sciences (39.99°N, 116.37°E) at ground level (~4 m), an urban site in the north of Beijing, as described by Sun et al. (2016). Sulfate concentrations in submicron aerosols (PM₁) were measured by an Aerodyne High Resolution Aerosol Mass Spectrometer (HR-AMS). The difference of SO₄²⁻ concentration between PM_{2.5} and PM₁ is small because most sulfate exists in fine aerosols (Guo et al., 2014). A comparison of SO₄²⁻ concentration in PM_{2.5} and PM₁ during 22 November – 29 November
40 2017 is shown in the supplement (Figure S2). Surface PM_{2.5}, SO₂, NO₂, and O₃ measurements (Figures 1 and S5) are from the China National Environmental Monitoring Center (<http://106.37.208.233:20035/>) with 12 sites in Beijing, including 8 urban and 4 suburban sites.

3 Results

45 3.1 Observed PM_{2.5} and sulfate concentrations and $\Delta^{17}\text{O}(\text{SO}_4^{2-})$

Figure 1 shows the time series of observed concentrations of PM_{2.5} and sulfate from 17 October 2014 to 20 January 2015, along with temperature and relative humidity in Beijing from GEOS-FP. A previous study showed that the GEOS-FP meteorological data for temperature and relative humidity are in good agreement with the ground-based measurements in Beijing ($R^2 > 0.9$) (Zhang et al., 2016). The CNAAQs defines the 24h average air quality levels as excellent (PM_{2.5} = 0-35
50 $\mu\text{g m}^{-3}$), good (PM_{2.5} = 35-75 $\mu\text{g m}^{-3}$), light (PM_{2.5} = 75-115 $\mu\text{g m}^{-3}$), moderate (PM_{2.5} = 115-150 $\mu\text{g m}^{-3}$), heavy (PM_{2.5} = 150-250 $\mu\text{g m}^{-3}$), and severe (PM_{2.5} > 250 $\mu\text{g m}^{-3}$). Using this metric, 10 time periods are categorized as heavy or severe (>150 $\mu\text{g m}^{-3}$) during 17 October 2014 – 20 January 2015, and we refer to these as “Heavy Polluted Period” (HPP). Another 10 time periods were in the excellent to good category and we refer to these days as “Clean Period” (CP). The average relative humidity (RH) from GEOS-FP during HPP was 60±11%, much higher than the average RH during CP



:55 (42±10%). Higher RH can accelerate the rates of conversion of SO₂ and NO₂ to SO₄²⁻ and NO₃⁻, respectively, contributing to increases in PM_{2.5} concentrations (Wang et al., 2016; Hua et al., 2015).

The observed SO₄²⁻ concentrations show a similar variation as PM_{2.5}, increasing from 2.1±1.8 μg m⁻³ in CP to 25.9±11.3 μg m⁻³ in HPP with a mean of 11.5±7.3 μg m⁻³ during the entire measurement period. The mass fraction of SO₄²⁻ to PM_{2.5} ranged from 5% to 19%, varying from a mean of 8±2% in CP to 13±2% in HPP. Observed sulfate concentrations shown in
:60 Figure 1 are 15% lower on average during HPP than those reported in He et al. (2018) because the SO₄²⁻ concentrations shown here represent PM₁ instead of PM_{2.5}, which is in good agreement with previous studies (Sun et al., 2013; 2014; 2016) (Fig. S2). Figure 1 also shows the observed sulfur oxidation ratio (SOR), defined as the molar ratio of sulfate over the sum of sulfate and SO₂ (SO₄²⁻/(SO₂ + SO₄²⁻)) (Colbeck and Harrison, 1984). The observed SOR increases from CP (9±6%) to
:65 HPP (32±18%), consistent with increased sulfate production rates during HPP.

Figures 2 and S4 show the Δ¹⁷O(SO₄²⁻) observations, 24 measurements represent HPP and 10 represent CP. The Δ¹⁷O(SO₄²⁻) values are similar in HPP and CP, 0.9±0.1‰ and 0.9±0.5‰, respectively. A more detailed description of the Δ¹⁷O(SO₄²⁻) observations can be found in He et al. (2018).

:70

3.2 Analyses of sulfate formation pathways

3.2.1 Sulfate formation in the standard model

Figure 1 compares the measured and modeled PM_{2.5} and sulfate concentration in Beijing. The standard model (Run_Std) generally captures the temporal variations of PM_{2.5} and SO₄²⁻ observations during the entire sampling period, but underestimates the PM_{2.5} and SO₄²⁻ observations during HPP by 28% and 64%, respectively. Modeled sulfate
:75 concentrations increase from 1.5±1.2 μg m⁻³ in CP to 8.9±3.1 μg m⁻³ in HPP, which is a much smaller enhancement compared to observations (from 2.1±1.8 μg m⁻³ in CP to 25.9±11.3 μg m⁻³ in HPP). The model simulated sulfate mass fractions in PM_{2.5} are 8±2% in CP and 7±2% in HPP. The model fails to reproduce increases in observed sulfate mass fraction from CP (8±2%) to HPP (13±2%). This is consistent with previous modeling studies, suggesting missing sulfate
:80 formation pathways (Wang et al., 2014; Zhang et al., 2015). The model also underestimates the sulfur oxidation ratio (SOR) observations during HPP by 53%. This further suggests that the modeled SO₂ oxidation rate is too slow.

Figure 2 compares observed and modeled Δ¹⁷O(SO₄²⁻). The modeled hourly Δ¹⁷O (SO₄²⁻) values were averaged at 12h intervals for comparison with the observations. The simulated Δ¹⁷O(SO₄²⁻) values in Run_Std range from 0.02‰ to 1.5‰ with a mean of 0.5±0.1‰. Unlike the observations, modeled Δ¹⁷O (SO₄²⁻) values in Run_Std during HPP (0.4±0.1‰) are
:85 lower than those during CP (0.6±0.1‰) due to higher fractional contribution of in-cloud H₂O₂ and O₃ oxidation pathways during CP, as discussed below. Run_Std underestimates the Δ¹⁷O(SO₄²⁻) observations (by 44% on average), particularly



during HPP (by 53% on average).

90 Figure 3 shows modeled spatial distribution of sulfate concentrations over China, and the fractional contribution of each sulfate formation pathway to total sulfate abundance in Beijing. The average simulated sulfate concentration in Beijing in Run_Std is around $6.2 \mu\text{g m}^{-3}$ (Figure 3a), smaller than the observations ($11.5 \mu\text{g m}^{-3}$) over the study period. Figure 3 also shows the model calculated average contribution of each sulfate production pathway to total sulfate concentration at the surface in Beijing during HPP and CP. In Run_Std, sulfate produced by gas-phase oxidation of SO_2 by OH dominates the total sulfate abundance (59.7%, $5.3 \mu\text{g m}^{-3}$) in HPP. Primary sulfate represents the second most important contributor (33.6%, $3.0 \mu\text{g m}^{-3}$) despite the fact that primary sulfate is only 3% of total anthropogenic sulfur emissions. The high fraction of primary anthropogenic sulfate reflects the relatively slow oxidation rate of SO_2 in the model. In-cloud sulfate production contributes only 7% of total sulfate abundance at the surface during HPP. For clean days, primary sulfate dominates surface sulfate concentrations (49.4%, $0.7 \mu\text{g m}^{-3}$), suggesting an even slower SO_2 oxidation rate in the model during CP compared to HPP. Gas-phase production via OH oxidation is the second most important contributor (26.1%, $0.4 \mu\text{g m}^{-3}$) during CP. Gas-phase oxidation of SO_2 by OH is more important in HPP than in CP because modeled OH concentrations during HPP are much higher than in CP, consistent with observations of high OH during polluted wintertime conditions in Beijing (Tan et al., 2018). Higher modeled OH in HPP compared to CP is due to higher nitrous acid (HONO) levels during HPP (Figure S3) resulting from heterogeneous uptake of NO_2 to produce HNO_3 and HONO in the model. This is consistent with observation-based studies in Beijing showing that OH production from HONO photolysis is 10 times higher than that from O_3 photolysis in winter (Hendrick et al., 2014) and that $\text{NO}_2(\text{g})$ dissolution in acidic aerosol water is a source of HONO (Li et al., 2018). In-cloud sulfate production contributes 24.5% of total sulfate abundance during CP, much higher than HPP (6.9%) due to higher modeled H_2O_2 and O_3 in CP.

10 3.2.2 Transition metal ion catalyzed oxidation of S(IV) in clouds

The in-cloud concentration of soluble Fe^{3+} and Mn^{2+} determines the rate of sulfate formation via the TMI-catalyzed oxidation pathway, but large uncertainties exist in estimates of soluble Fe^{3+} and Mn^{2+} due to lack of observations. Adding aqueous-phase TMI-catalyzed S(IV) oxidation by O_2 in cloud droplets in Run_TMI increases the average sulfate concentration in Beijing during the entire measurement period from $6.2 \mu\text{g m}^{-3}$ to $8.3 \mu\text{g m}^{-3}$ due to increases in the in-cloud sulfate production rate. However, the model still underestimates observations of $\text{PM}_{2.5}$ (-35%), sulfate (-48%), and SOR (-40%) during HPP. Sulfate from TMI-catalyzed oxidation dominates in-cloud sulfate production and accounts for up to 28.3% of total sulfate abundance during HPP, but only 8.1% during CP in Beijing (Figure 3b). The lower contribution of TMI-catalysis during CP is due to lower concentrations of Fe and Mn in the model during CP. The largest enhancement in sulfate abundance after adding the in-cloud TMI pathway occurs in Sichuan basin (around $6.5 \mu\text{g m}^{-3}$), where simulated anthropogenic Fe and Mn from coal fly ash and SO_2 are high (Zhang et al., 2009) in part due to stagnant air and high



relative humidity all year (Huang et al., 2014). After adding the in-cloud TMI oxidation pathway, the average modeled $\Delta^{17}\text{O}(\text{SO}_4^{2-})$ decreased from 0.5‰ to 0.4‰ in Beijing because the TMI oxidation pathway leads to $\Delta^{17}\text{O}(\text{SO}_4^{2-}) = 0\text{‰}$ (Figure 2), which makes the discrepancy between modeled and observed $\Delta^{17}\text{O}(\text{SO}_4^{2-})$ (0.9 ‰) even larger.

25 3.2.3 Heterogeneous sulfate formation on aerosols

Adding four heterogeneous S(IV) oxidation mechanisms by H_2O_2 , O_3 , NO_2 and TMI-catalyzed O_2 on aerosols in Run_Het increases the average SO_4^{2-} concentrations in Beijing (from $8.3 \mu\text{g m}^{-3}$ in Run_Std to $9.8 \mu\text{g m}^{-3}$ in Run_Het) (Figure 1c). Modeled heterogeneous sulfate production represents 21.6% of total surface sulfate concentrations in HPP and 19.8% in CP (Figure 3c). Modeled daily-mean aerosol pH ranged from 3.0 to 5.4 with a mean of 4.3 over the entire time period in Beijing (Figure 4), which is consistent with recent estimates (pH=4.2-4.7) (Guo et al, 2017; Song et al, 2018a; Liu et al., 2017). Heterogeneous sulfate production on aerosols is dominated by TMI-catalyzed O_2 oxidation in both HPP (69%) and CP (67%) (Figure 3c). S(IV) oxidation by O_3 is the second most important heterogeneous oxidation pathway, accounting for 19% of total heterogeneous sulfate formation in both HPP and CP. S(IV) oxidation by H_2O_2 (6% in both HPP and CP) and NO_2 (6% in HPP and 8% in CP) represent a minor heterogeneous sulfate production pathway. Previous studies suggested that oxidation of SO_2 by NO_2 in aerosol water dominates heterogeneous sulfate formation in Beijing during winter (Wang et al., 2016; Cheng et al., 2016) at neutral aerosol pH. However, subsequent studies showed that these high aerosol pH values were unlikely during wintertime Beijing haze events and they calculated aerosol pH values in the range of 4.2-4.7 (Guo et al, 2017; Song et al, 2018a; Liu et al., 2017).

After adding the heterogeneous S(IV) oxidation pathways, the average modeled $\Delta^{17}\text{O}(\text{SO}_4^{2-})$ increased from $0.5 \pm 0.5\text{‰}$ to $0.8 \pm 0.7\text{‰}$ in Beijing due to the increased importance of S(IV) oxidation by O_3 . Although the average modeled $\Delta^{17}\text{O}(\text{SO}_4^{2-})$ in Run_Het is similar to the observations ($0.9 \pm 0.3\text{‰}$), the modeled median (0.5‰) largely underestimates the observed median (1.0‰) (Figure 2), and the majority of the modeled data underestimates the observed $\Delta^{17}\text{O}(\text{SO}_4^{2-})$ (Figure S4).

Compared to observations in Beijing, mean model biases decrease from -28% to -26% for $\text{PM}_{2.5}$, -45% to -21% for sulfate concentration, from -29% to -11% for SOR, and from -45% to -15% for $\Delta^{17}\text{O}(\text{SO}_4^{2-})$ for the entire measurement period for Run_Het relative to Run_Std. Model biases during HPP decrease from -38% to -32% for $\text{PM}_{2.5}$, -65% to -40% for sulfate concentration, -53% to -28% for SOR, and from -50% to -5% for $\Delta^{17}\text{O}(\text{SO}_4^{2-})$. The largest sulfate enhancements due to heterogeneous sulfate formation occur in megacities in eastern China and Sichuan basin (Figure 3), where both SO_2 and aerosols abundances are highest. In addition, high anthropogenic emissions of Fe^{3+} and Mg^{2+} favor sulfate production catalyzed by TMIs. In Run_Het, the fractional contribution of each sulfate production mechanism in Beijing during HPP is 34% for gas-phase oxidation of SO_2 by OH, 22% for TMI-catalysis in cloud, 21% for the four heterogeneous oxidation pathways, and 20% for primary sulfate, respectively (Figure 3c). The remaining 3% of sulfate is formed via in-cloud sulfate



production from H₂O₂ and O₃. For clean days (CP), primary sulfate still dominates surface sulfate concentrations (39%) in
Run_Het, with gas-phase production via OH oxidation the second most important contributor (22%) and the added
heterogeneous sulfate formation pathways accounting for 22%.

4. Discussion

The model results demonstrate that implementation of heterogeneous sulfate formation pathways on aerosols reduces
modeled low biases in both concentration and oxygen isotopic signature of sulfate ($\Delta^{17}\text{O}(\text{SO}_4^{2-})$), and suggests that
TMI-catalysis dominates heterogeneous sulfate production. However, the model is still biased low in both metrics,
indicating that the model is still underestimating sulfate production rates. The modeled underestimate in $\Delta^{17}\text{O}(\text{SO}_4^{2-})$
reveals an underestimate in the O₃ oxidation pathway. Since the relative contribution of heterogeneous sulfate formation
pathways are sensitive to aerosol pH, we investigated the influence of aerosol pH using a series of sensitivity simulations
with prescribed aerosol pH values between 2 and 8 (Table 1). Figure 5 shows modeled sulfate concentrations produced
from different oxidation pathways and resulting $\Delta^{17}\text{O}(\text{SO}_4^{2-})$ in Beijing averaged over HPP assuming different aerosol pH
values. Heterogeneous sulfate formation represents over 50% of total sulfate formation when pH > 5 and when pH < 4. At
aerosol pH < 4, heterogeneous sulfate formation is dominated by the TMI pathway because of the high solubility of Fe and
Mn at low pH (Guieu et al. 1994, Mackie, et al. 2005). At aerosol pH > 5, heterogeneous sulfate formation is dominated by
the O₃ pathway because the solubility of SO₂ increases with increasing pH and because the S(IV) partitioning shifts to
favor SO₃²⁻ at higher pH. The aqueous-phase rate constant for SO₃²⁻ + O₃ is almost four orders of magnitude faster than for
HSO₃⁻ + O₃ (Table S2). Heterogeneous sulfate formation by NO₂ also increases with increasing pH due to the increased
solubility of SO₂ at high pH, and represents 15-30% of total heterogeneous sulfate production between pH = 6 – 8. In
contrast to our results, previous results (Cheng et al., 2016; Wang et al., 2016) suggested that NO₂ oxidation is more
important than O₃ oxidation at high pH values. The difference is due to assumed O₃ concentrations used in the rate
calculations. The aforementioned studies assumed an O₃ concentration of 1 ppb relative to an NO₂ concentration of 66 ppb.
In our model simulations, average O₃ and NO₂ concentrations are 9 ppb and 85 ppb, respectively. Modeled O₃
concentrations are similar to the observations during the measurement period (Figure S5). Heterogeneous sulfate
production is lower (20%) when pH = 4 - 5 because of the low solubility of Fe and Mn and low concentrations of SO₃²⁻ in
this pH range. We note that while the pH-dependence of S(IV) partitioning is well known, the pH-dependency of metal
solubility is more uncertain.

Figure 5 also shows that model results with mean aerosol pH > 5 would result in a high bias in $\Delta^{17}\text{O}(\text{SO}_4^{2-})$ due to the
increasing importance of the O₃ oxidation pathway at higher pH values, effectively providing an observational constraint
for typical aerosol pH < 5 in Beijing haze. However, modeled $\Delta^{17}\text{O}(\text{SO}_4^{2-})$ calculated at the aerosol pH of 4.2-4.7 as
estimated by recent studies (Guo et al. 2017; Song et al. 2018a) represents a low bias relative to the observations. A joint



comparison of observations and model results with both sulfate concentrations and $\Delta^{17}\text{O}$ (SO_4^{2-}) suggests an average aerosol pH between 5-6 in Beijing during the study period, which is higher than bulk aerosol pH calculations in our model calculations and in previous studies (Guo et al. 2017; Song et al. 2018a).

90

Thermodynamic pH calculations in ISORROPIA II are based on the assumption of internally mixed aerosols and do not directly consider aerosol alkalinity (carbonate). Fresh dust is initially alkaline (calcium carbonates). This alkalinity is partially depleted (carbonate is converted to CO_2) upon uptake of acid gases HNO_3 , SO_2 , and H_2SO_4 (Fairlie et al, 2010; Usher et al., 2003). Due to the high pH of alkaline dust, uptake of SO_2 would be followed by heterogeneous oxidation by O_3 (Fairlie et al., 2010; Ullerstam et al., 2003) and NO_2 (Zhao et al., 2018) if there is enough aerosol liquid water to promote aqueous-phase oxidation. A recent modeling study by Uno et al. (2017) using a previous version of GEOS-Chem explicitly includes uptake of HNO_3 , SO_2 , and H_2SO_4 on alkaline dust aerosols as described in Fairlie et al. (2010). Their model calculated that sulfate from uptake of SO_2 and H_2SO_4 on alkaline dust in Beijing during our measurement period represents on average 3% of total sulfate abundance. Most of this sulfate formation on alkaline dust was from uptake of H_2SO_4 (70 – 80%, Fairlie et al., 2010), with the remaining fraction (20 – 30%) from uptake of SO_2 followed by oxidation to sulfate. On average, less than 1% of sulfate in Beijing is formed on alkaline dust via the uptake and oxidation of SO_2 in the model.

95

100

105

110

115

At pH values representative of alkaline dust ($\text{pH} = 7 - 8$), sulfate formed via oxidation of SO_2 on alkaline dust would be dominated by O_3 leading to a relatively high $\Delta^{17}\text{O}(\text{SO}_4^{2-})$ value of 6‰ (Figure 5). In order to account for the difference in the median $\Delta^{17}\text{O}(\text{SO}_4^{2-})$ observed (1.0‰) and modeled (0.5‰), sulfate formation from the uptake and oxidation of SO_2 on alkaline dust would need to account for an average of 9% of total sulfate abundance during our measurement period. This fraction is higher than that calculated in Uno et al. (2017), which did not include anthropogenic dust. In our model, anthropogenic dust accounts for 12% of total dust, which is not enough to explain the difference. Due to uncertainties in processes such as the RH dependence of the uptake of SO_2 on alkaline dust, the importance of this pathway could be underestimated in Uno et al. (2017). If this process does account for the difference in modeled and observed $\Delta^{17}\text{O}(\text{SO}_4^{2-})$, then NO_2 oxidation may be slightly more important than indicated in Figure 3. Our calculations (Figure 5) suggest that NO_2 oxidation accounts for 23% of heterogeneous sulfate formation at aerosol pH values between 7 and 8. If sulfate formation on alkaline dust accounts for 9% of total sulfate formation, and NO_2 oxidation accounts for 23% of this sulfate formation pathway, then NO_2 oxidation can account for up to 2% of total heterogeneous sulfate formation in Beijing, which still suggests NO_2 oxidation is a minor pathway during wintertime Beijing haze events.

120

An increase in sulfate abundance of 9% from formation on alkaline dust is not enough to explain the remaining model underestimate in sulfate concentrations (-40%) and SOR (-28%) during HPP. Two recent studies suggested that hydroxymethane sulfonate (HMS) may be present in Chinese haze events and measured as sulfate via ion chromatography



and HR-AMS (Moch et al., 2018; Song et al., 2018b). HMS is formed via aqueous-phase oxidation via nucleophilic attack of HSO_3^- and SO_3^{2-} on HCHO. Moch et al. (2018) suggested that in-cloud formation of HMS could explain the low model bias in sulfate concentrations, while Song et al. (2018b) suggested that heterogeneous formation of HMS on aerosol surfaces can explain up to one-third of the low model bias in their study. In the present study, as the organics were removed from the sample matrix prior to $\Delta^{17}\text{O}(\text{SO}_4^{2-})$ analysis (Geng et al., 2013), it is unlikely that measured $\Delta^{17}\text{O}(\text{SO}_4^{2-})$ have significant contributions from HMS. However, the presence of HMS in the sample matrix, if any, would lower measured $\Delta^{17}\text{O}(\text{SO}_4^{2-})$, and any correction for this would increase the observed $\Delta^{17}\text{O}(\text{SO}_4^{2-})$ and further increase the discrepancy between modeled and observed $\Delta^{17}\text{O}(\text{SO}_4^{2-})$.

5. Conclusion

We have used a combination of observations and modeling of sulfate and SO_2 concentrations and $\Delta^{17}\text{O}(\text{SO}_4^{2-})$ to quantify sulfate production mechanisms in Beijing. We focus on the period of 17 October 2014 – 20 January 2015, when 10 heavy pollution periods (HPP) were defined with observed $\text{PM}_{2.5}$ concentrations $>150 \mu\text{g m}^{-3}$. The standard model simulation that only includes primary sulfate and sulfate formation from gas-phase oxidation by OH and in-cloud oxidation by H_2O_2 and O_3 underestimates mean sulfate concentration by 65% and $\Delta^{17}\text{O}(\text{SO}_4^{2-})$ by 50% during heavy pollution periods (HPP). Adding in-cloud oxidation catalyzed by transition metal ions (TMI) and heterogeneous oxidation by H_2O_2 , O_3 , NO_2 , and TMI on aerosols can improve the model simulation of sulfate abundance and $\Delta^{17}\text{O}(\text{SO}_4^{2-})$, with the model biases decreasing from -65% to -40% for sulfate and from -50% to -5% for $\Delta^{17}\text{O}(\text{SO}_4^{2-})$ during HPP. Modeled heterogeneous sulfate production accounts for around 20% of total sulfate production. The TMI-catalyzed oxidation dominates heterogeneous sulfate production under calculated aerosol pH of ≤ 5 ; however, the modeled $\Delta^{17}\text{O}(\text{SO}_4^{2-})$ is still biased low compared to observations, suggesting an underestimate of sulfate production by O_3 oxidation. We hypothesize that sulfate aerosol production by O_3 on externally-mixed alkaline dust aerosol can explain the remaining discrepancy in $\Delta^{17}\text{O}(\text{SO}_4^{2-})$. The $\Delta^{17}\text{O}(\text{SO}_4^{2-})$ observations suggest that a fractional sulfate contribution of just 9% originating from SO_2 oxidation on alkaline dust aerosol can explain the model discrepancy in $\Delta^{17}\text{O}(\text{SO}_4^{2-})$. We calculate that sulfate formation on alkaline dust is dominated by O_3 oxidation (74%) followed by NO_2 oxidation (23%). The $\Delta^{17}\text{O}(\text{SO}_4^{2-})$ observations combined with our model calculations indicates only a minor (2%) role of heterogeneous sulfate formation via NO_2 oxidation of SO_2 . Future studies will examine the impact of these heterogeneous S(IV) oxidation mechanisms on the regional and global sulfur budgets.

Data availability

For the model results please contact Becky Alexander (beckya@uw.edu) and Lin Zhang (zhanglg@pku.edu.cn). For isotope measurements please contact Zhouqing Xie (zqxie@ustc.edu.cn)



Author contribution

55 BA, LZ and JYS designed the study. BA and LZ supervised the project. JYS performed model simulations and conducted analyses with the assistance of QJC, YXW, XL, VS, RVM, SP, SJS and YZ. ZQX and PZH conducted the oxygen isotope measurements; YLS contributed the sulfate measurements. BA, LZ and JYS wrote the paper. All authors contributed to the interpretation of the results and improvement of the paper.

60 Acknowledgements

This work is supported by the National Key Research and Development Program of China (2017YFC0210102) and the National Natural Science Foundation of China (41475112). J.Y. Shao acknowledges support from the Chinese Scholarship Council. B.A. Acknowledges support from NSF AGS 1644998 and Y. W. acknowledge support from NSF AGS 1645062. Z.Q.Xie acknowledges support from the National Natural Science Foundation of China (91544013). We thank Duncan
65 Fairlie, Itushi Uno, Renyi Zhang, Havala O.T.Pye, ISHINO Sakiko, HATTORI Shohei, Youfan Chen, Jessica Haskins, Mi Zhou for helpful discussions.

References

- 70 Alexander, B., R. J. Park, D. J. Jacob, Q. B. Li, R. M. Yantosca, J. Savarino, C. C. W. Lee, and M. H. Thiemens: Sulfate formation in sea-salt aerosols: Constraints from oxygen isotopes, *J. Geophys. Res.*, 110, D10307, doi:10.1029/2004jd005659, 2005.
- Alexander, B., Hastings, M. G., Allman, D. J., Dachs, J., Thornton, J. A., and Kunasek, S. A.: Quantifying atmospheric nitrate formation pathways based on a global model of the oxygen isotopic composition ($\Delta^{17}\text{O}$) of atmospheric nitrate, *Atmos. Chem. Phys.*, 9, 5043-5056, doi:10.5194/acp-9-5043-2009, 2009.
- 75 Alexander, B., Allman, D. J., Amos, H. M., Fairlie, T. D., Dachs, J., Hegg, D. A., and Sletten, R. S.: Isotopic constraints on the formation pathways of sulfate aerosol in the marine boundary layer of the subtropical northeast Atlantic Ocean, *J. Geophys. Res.*, 117, D06304, doi:10.1029/2011jd016773, 2012.
- Ammann, M., Cox, R. A., Crowley, J. N., Jenkin, M. E., Mellouki, A., Rossi, M. J., Troe, J., and Wallington, T. J.:
80 Evaluated kinetic and photochemical data for atmospheric chemistry: Volume VI – heterogeneous reactions with liquid substrates, *Atmos. Chem. Phys.*, 13, 8045-8228, doi:10.5194/acp-13-8045-2013, 2013.
- Beijing Environment Protection Agency: The report for 2017 air quality in Beijing, 2018 (<http://www.bjepb.gov.cn/bjhrb/index/index.html> (in Chinese))
- Calvert, J. G., and Stockwell, W. R.: Acid generation in the troposphere by gas-phase chemistry, *Environ. Sci. Technol.*, 17, 428A-443A, doi:10.1021/es00115a727, 1983.
- 85 Chen, D., Liu, Z., Fast, J., and Ban, J.: Simulations of sulfate–nitrate–ammonium (SNA) aerosols during the extreme haze events over northern China in October 2014, *Atmos. Chem. Phys.*, 16, 10707-10724, doi:10.5194/acp-16-10707-2016, 2016.
- Chen, Q., Geng, L., Schmidt, J. A., Xie, Z., Kang, H., Dachs, J., Cole-Dai, J., Schauer, A. J., Camp, M. G., and Alexander,



- 90 B.: Isotopic constraints on the role of hypohalous acids in sulfate aerosol formation in the remote marine boundary layer, *Atmos. Chem. Phys.*, 16, 11433-11450, doi:10.5194/acp-16-11433-2016, 2016.
- Chen, Q., Schmidt, J. A., Shah, V., Jaeglé, L., Sherwen, T., and Alexander, B.: Sulfate production by reactive bromine: Implications for the global sulfur and reactive bromine budgets, *Geophys. Res. Lett.*, 44, 7069-7078, doi:10.1002/2017gl073812, 2017.
- Chen, Q., Sherwen, T., Evans, M., and Alexander, B.: DMS oxidation and sulfur aerosol formation in the marine troposphere: a focus on reactive halogen and multiphase chemistry, *Atmos. Chem. Phys.*, 18, 13617-13637, doi:10.5194/acp-18-13617-2018, 2018.
- 95 Cheng, Y., Zheng, G., Wei, C., Mu, Q., Zheng, B., Wang, Z., Gao, M., Zhang, Q., He, K., Carmichael, G., Poschl, U., and Su, H.: Reactive nitrogen chemistry in aerosol water as a source of sulfate during haze events in China, *Sci. Adv.*, 2, e1601530, doi:10.1126/sciadv.1601530, 2016.
- 100 Chinese State Council. Atmospheric Pollution Prevention and Control Action Plan (http://www.gov.cn/zwggk/2013-09/12/content_2486773.htm (in Chinese)), last access on 12/01/2018)
- Chuang, P. Y., Duvall, R. M., Shafer, M. M., and Schauer, J. J.: The origin of water soluble particulate iron in the Asian atmospheric outflow, *Geophys. Res. Lett.*, 32, L07813, doi:10.1029/2004gl021946, 2005.
- Colbeck, I., and Harrison, R.: Ozone—secondary aerosol—visibility relationships in North-West England, *Sci. Total Environ.*, 34, 87-100, doi:10.1016/0048-9697(84)90043-3, 1984.
- 105 Desboeufs, K. V., Losno, R., and Colin, J. L.: Factors influencing aerosol solubility during cloud processes, *Atmos. Environ.*, 35, 3529-3537, doi:10.1016/s1352-2310(00)00472-6, 2001.
- Desboeufs, K. V., Sofikitis, A., Losno, R., Colin, J. L., and Ausset, P.: Dissolution and solubility of trace metals from natural and anthropogenic aerosol particulate matter, *Chemosphere*, 58, 195-203, doi:10.1016/j.chemosphere.2004.02.025, 2005.
- 110 Dominguez, G., Jackson, T., Brothers, L., Barnett, B., Nguyen, B., and Thiemens, M. H.: Discovery and measurement of an isotopically distinct source of sulfate in Earth's atmosphere, *Proc. Natl. Acad. Sci.*, 105, 12769-12773, doi:10.1073/pnas.0805255105, 2008.
- Dubey, M. K., Mohrschladt, R., Donahue, N. M., and Anderson, J. G.: Isotope Specific Kinetics of Hydroxyl Radical (OH) with Water (H₂O): Testing Models of Reactivity and Atmospheric Fractionation, *J. Phys. Chem.*, 101, 1494-1500, doi:10.1021/jp962332p, 1997.
- 115 Fairlie, T. D., Jacob, D. J., and Park, R. J.: The impact of transpacific transport of mineral dust in the United States, *Atmos. Environ.*, 41, 1251-1266, doi:10.1016/j.atmosenv.2006.09.048, 2007.
- Fairlie, T. D., Jacob, D. J., Dibb, J. E., Alexander, B., Avery, M. A., van Donkelaar, A., and Zhang, L.: Impact of mineral dust on nitrate, sulfate, and ozone in transpacific Asian pollution plumes, *Atmos. Chem. Phys.*, 10, 3999-4012, doi:10.5194/acp-10-3999-2010, 2010.
- 120 Fountoukis, C., and Nenes, A.: ISORROPIA II: a computationally efficient thermodynamic equilibrium model for K⁺-Ca²⁺-Mg²⁺-NH₄⁺-Na⁺-SO₄²⁻-NO₃⁻-Cl⁻-H₂O aerosols, *Atmos. Chem. Phys.*, 7, 4639-4659, doi:10.5194/acp-7-4639-2007, 2007.



- 25 Gao, M., Guttikunda, S. K., Carmichael, G. R., Wang, Y., Liu, Z., Stanier, C. O., Saide, P. E., and Yu, M.: Health impacts and economic losses assessment of the 2013 severe haze event in Beijing area, *Sci. Total Environ.*, 511, 553-561, doi:10.1016/j.scitotenv.2015.01.005, 2015.
- Gao, M., Carmichael, G. R., Saide, P. E., Lu, Z., Yu, M., Streets, D. G., and Wang, Z.: Response of winter fine particulate matter concentrations to emission and meteorology changes in North China, *Atmos. Chem. Phys.*, 16, 11837-11851, doi:10.5194/acp-16-11837-2016, 2016.
- 30 Geng, G., Zhang, Q., Martin, R. V., Lin, J., Huo, H., Zheng, B., Wang, S., and He, K.: Impact of spatial proxies on the representation of bottom-up emission inventories: A satellite-based analysis, *Atmos. Chem. Phys.*, 17, 4131-4145, doi:10.5194/acp-17-4131-2017, 2017.
- Geng, L., Schauer, A. J., Kunasek, S. A., Sofen, E. D., Erbland, J., Savarino, J., Allman, D. J., Sletten, R. S., and Alexander, B.: Analysis of oxygen-17 excess of nitrate and sulfate at sub-micromole levels using the pyrolysis method, *Rapid Commun. Mass Sp.*, 27, 2411-2419, doi:10.1002/rcm.6703, 2013.
- 35 Guieu, C., Duce, R., and Arimoto, R.: Dissolved input of manganese to the ocean: Aerosol source, *J. Geophys. Res.*, 99, 18789-18800, doi:10.1029/94jd01120, 1994.
- Guo, H., Weber, R. J., and Nenes, A.: High levels of ammonia do not raise fine particle pH sufficiently to yield nitrogen oxide-dominated sulfate production, *Sci. Rep.*, 7, 12109, doi:10.1038/s41598-017-11704-0, 2017.
- 40 Guo, S., Hu, M., Zamora, M. L., Peng, J., Shang, D., Zheng, J., Du, Z., Wu, Z., Shao, M., Zeng, L., Molina, M. J., and Zhang, R.: Elucidating severe urban haze formation in China, *Proc. Natl. Acad. Sci.*, 111, 17373-17378, doi:10.1073/pnas.1419604111, 2014.
- Harris, E., Sinha, B., van Pinxteren, D., Tilgner, A., Fomba, K. W., Schneider, J., Roth, A., Gnauk, T., Fahlbusch, B., Mertes, S., Lee, T., Collett, J., Foley, S., Borrmann, S., Hoppe, P., and Herrmann, H.: Enhanced Role of Transition Metal Ion Catalysis During In-Cloud Oxidation of SO₂, *Science*, 340, 727-730, doi:10.1126/science.1230911, 2013.
- 45 He, P., Alexander, B., Geng, L., Chi, X., Fan, S., Zhan, H., Kang, H., Zheng, G., Cheng, Y., Su, H., Liu, C., and Xie, Z.: Isotopic constraints on heterogeneous sulfate production in Beijing haze, *Atmos. Chem. Phys.*, 18, 5515-5528, doi:10.5194/acp-18-5515-2018, 2018.
- 50 Hendrick, F., Müller, J. F., Clémer, K., Wang, P., De Mazière, M., Fayt, C., Gielen, C., Hermans, C., Ma, J. Z., Pinardi, G., Stavrou, T., Vlemmix, T., and Van Roozendaal, M.: Four years of ground-based MAX-DOAS observations of HONO and NO₂ in the Beijing area, *Atmos. Chem. Phys.*, 14, 765-781, doi:10.5194/acp-14-765-2014, 2014.
- Hennigan, C. J., Izumi, J., Sullivan, A. P., Weber, R. J., and Nenes, A.: A critical evaluation of proxy methods used to estimate the acidity of atmospheric particles, *Atmos. Chem. Phys.*, 15, 2775-2790, doi:10.5194/acp-15-2775-2015, 2015.
- 55 Herrmann, H., Schaefer, T., Tilgner, A., Styler, S. A., Weller, C., Teich, M., and Otto, T.: Tropospheric aqueous-phase chemistry: kinetics, mechanisms, and its coupling to a changing gas phase, *Chem. Rev.*, 115, 4259-4334, doi:10.1021/cr500447k, 2015.
- Holt, B. D., Kumar, R., and Cunningham, P. T.: Oxygen-18 study of the aqueous-phase oxidation of sulfur dioxide, *Atmos. Environ.*, 15, 557-566, doi:10.1016/0004-6981(81)90186-4, 1981.
- 60



- Hua, Y., Cheng, Z., Wang, S., Jiang, J., Chen, D., Cai, S., Fu, X., Fu, Q., Chen, C., Xu, B., and Yu, J.: Characteristics and source apportionment of PM_{2.5} during a fall heavy haze episode in the Yangtze River Delta of China, *Atmos. Environ.*, 123, 380-391, doi:10.1016/j.atmosenv.2015.03.046, 2015.
- 65 Huang, X., Song, Y., Zhao, C., Li, M., Zhu, T., Zhang, Q., and Zhang, X.: Pathways of sulfate enhancement by natural and anthropogenic mineral aerosols in China, *J. Geophys. Res.: -Atmos.*, 119, 1165-1174, doi:10.1002/2014jd022301, 2014.
- Huie, R. E., and Neta, P.: Chemical behavior of SO₃⁻ and SO₅⁻ radicals in aqueous solutions, *J. Phys. Chem.*, 88, 5665-5669, doi:10.1021/j150667a042, 1984.
- 70 Hung, H. M., and Hoffmann, M. R.: Oxidation of Gas-Phase SO₂ on the Surfaces of Acidic Microdroplets: Implications for Sulfate and Sulfate Radical Anion Formation in the Atmospheric Liquid Phase, *Environ. Sci. Technol.*, 49, 13768-13776, doi:10.1021/acs.est.5b01658, 2015.
- Ishino, S., Hattori, S., Savarino, J., Jourdain, B., Preunkert, S., Legrand, M., Caillon, N., Barbero, A., Kuribayashi, K., and Yoshida, N.: Seasonal variations of triple oxygen isotopic compositions of atmospheric sulfate, nitrate, and ozone at Dumont d'Urville, coastal Antarctica, *Atmos. Chem. Phys.*, 17, 3713-3727, doi:10.5194/acp-17-3713-2017, 2017.
- 75 Jacob, D. J.: Heterogeneous chemistry and tropospheric ozone, *Atmos. Environ.*, 34, 2131-2159, doi:10.1016/s1352-2310(99)00462-8, 2000.
- Jenkins, K. A., and Bao, H.: Multiple oxygen and sulfur isotope compositions of atmospheric sulfate in Baton Rouge, *Atmos. Environ.*, 40, 4528-4537, doi:10.1016/j.atmosenv.2006.04.010, 2006.
- 80 Lee, C. C. W., and Thiemens, M. H.: The δ¹⁷O and δ¹⁸O measurements of atmospheric sulfate from a coastal and high alpine region: A mass-independent isotopic anomaly, *J. Geophys. Res.: -Atmos.*, 106, 17359-17373, doi:10.1029/2000jd900805, 2001.
- Lee, C. C. W., Savarino, J., and Thiemens, M. H.: Mass independent oxygen isotopic composition of atmospheric sulfate: Origin and implications for the present and past atmosphere of Earth and Mars, *Geophys. Res. Lett.*, 28, 1783-1786, doi:10.1029/2000gl011826, 2001.
- 85 Lelieveld, J., Evans, J. S., Fnais, M., Giannadaki, D., and Pozzer, A.: The contribution of outdoor air pollution sources to premature mortality on a global scale, *Nature*, 525, 367-371, doi:10.1038/nature15371, 2015.
- Li, G., Bei, N., Cao, J., Huang, R., Wu, J., Feng, T., Wang, Y., Liu, S., Zhang, Q., Tie, X., and Molina, L. T.: A possible pathway for rapid growth of sulfate during haze days in China, *Atmos. Chem. Phys.*, 17, 3301-3316, doi:10.5194/acp-17-3301-2017, 2017a.
- 90 Li, L., Hoffmann, M. R., and Colussi, A. J.: Role of Nitrogen Dioxide in the Production of Sulfate during Chinese Haze-Aerosol Episodes, *Environ. Sci. Technol.*, 52, 2686-2693, doi:10.1021/acs.est.7b05222, 2018.
- Li, M., Zhang, Q., Kurokawa, J.-i., Woo, J.-H., He, K., Lu, Z., Ohara, T., Song, Y., Streets, D. G., Carmichael, G. R., Cheng, Y., Hong, C., Huo, H., Jiang, X., Kang, S., Liu, F., Su, H., and Zheng, B.: MIX: a mosaic Asian anthropogenic emission inventory under the international collaboration framework of the MICS-Asia and HTAP, *Atmos. Chem. Phys.*, 17, 935-963, doi:10.5194/acp-17-935-2017, 2017b.
- 95 Li, W., Zhou, S., Wang, X., Xu, Z., Yuan, C., Yu, Y., Zhang, Q., and Wang, W.: Integrated evaluation of aerosols from



- regional brown hazes over northern China in winter: Concentrations, sources, transformation, and mixing states, *J. Geophys. Res.*, 116, D09301, doi:10.1029/2010jd015099, 2011.
- i00 Liu, H., Jacob, D. J., Bey, I., and Yantosca, R. M.: Constraints from ^{210}Pb and ^7Be on wet deposition and transport in a global three-dimensional chemical tracer model driven by assimilated meteorological fields, *J. Geophys. Res.: -Atmos.*, 106, 12109-12128, doi:10.1029/2000jd900839, 2001.
- Liu, M., Song, Y., Zhou, T., Xu, Z., Yan, C., Zheng, M., Wu, Z., Hu, M., Wu, Y., and Zhu, T.: Fine particle pH during severe haze episodes in northern China, *Geophys. Res. Lett.*, 44, 5213-5221, doi:10.1002/2017gl073210, 2017.
- i05 Liu, Z., Hu, B., Wang, L., Wu, F., Gao, W., and Wang, Y.: Seasonal and diurnal variation in particulate matter (PM_{10} and $\text{PM}_{2.5}$) at an urban site of Beijing: analyses from a 9-year study, *Environ. Sci. Pollut. Res. Int.*, 22, 627-642, doi:10.1007/s11356-014-3347-0, 2015.
- Ma, Q., Cai, S., Wang, S., Zhao, B., Martin, R. V., Brauer, M., Cohen, A., Jiang, J., Zhou, W., Hao, J., Frostad, J., Forouzanfar, M. H., and Burnett, R. T.: Impacts of coal burning on ambient $\text{PM}_{2.5}$ pollution in China, *Atmos. Chem. Phys.*, 17, 4477-4491, doi:10.5194/acp-17-4477-2017, 2017.
- i10 Mackie, D. S.: Simulating the cloud processing of iron in Australian dust: pH and dust concentration, *Geophys. Res. Lett.*, 32, L06809, doi:10.1029/2004gl022122, 2005.
- McCabe, J. R., Savarino, J., Alexander, B., Gong, S., and Thiemens, M. H.: Isotopic constraints on non-photochemical sulfate production in the Arctic winter, *Geophys. Res. Lett.*, 33, L05810, doi:10.1029/2005gl025164, 2006.
- Moch, J. M., Dovrou, E., Mickley, L. J., Keutsch, F. N., Cheng, Y., Jacob, D. J., Jiang, J., Li, M., Munger, J. W., Qiao, X., and Zhang, Q.: Contribution of Hydroxymethane Sulfonate to Ambient Particulate Matter: A Potential Explanation for High Particulate Sulfur During Severe Winter Haze in Beijing, *Geophys. Res. Lett.*, 45, 11,969- 11,979, doi:10.1029/2018gl079309, 2018.
- i15 Park, R. J.: Natural and transboundary pollution influences on sulfate-nitrate-ammonium aerosols in the United States: Implications for policy, *J. Geophys. Res.*, 109, D15204, doi:10.1029/2003jd004473, 2004.
- i20 Patris, N., Cliff, S. S., Quinn, P. K., Kasem, M., and Thiemens, M. H.: Isotopic analysis of aerosol sulfate and nitrate during ITCT-2k2: Determination of different formation pathways as a function of particle size, *J. Geophys. Res.*, 112, D23301, doi:10.1029/2005jd006214, 2007.
- Philip, S., Martin, R. V., Snider, G., Weagle, C. L., van Donkelaar, A., Brauer, M., Henze, D. K., Klimont, Z., Venkataraman, C., Guttikunda, S. K., and Zhang, Q.: Anthropogenic fugitive, combustion and industrial dust is a significant, underrepresented fine particulate matter source in global atmospheric models, *Environ. Res. Lett.*, 12, 044018, doi:10.1088/1748-9326/aa65a4, 2017.
- i25 Pye, H. O. T., Liao, H., Wu, S., Mickley, L. J., Jacob, D. J., Henze, D. K., and Seinfeld, J. H.: Effect of changes in climate and emissions on future sulfate-nitrate-ammonium aerosol levels in the United States, *J. Geophys. Res.: -Atmos.*, 114, D01205, doi:10.1029/2008jd010701, 2009.
- i30 Ravishankara, A. R.: Heterogeneous and Multiphase Chemistry in the Troposphere, *Science*, 276, 1058-1065, doi:10.1126/science.276.5315.1058, 1997.
- Savarino, J., Lee, C. C. W., and Thiemens, M. H.: Laboratory oxygen isotopic study of sulfur (IV) oxidation: Origin of the



- mass-independent oxygen isotopic anomaly in atmospheric sulfates and sulfate mineral deposits on Earth, *Journal of Geophysical Research: Atmospheres*, 105, 29079-29088, [10.1029/2000jd900456](https://doi.org/10.1029/2000jd900456), 2000.
- i35 Shen, Z., Sun, J., Cao, J., Zhang, L., Zhang, Q., Lei, Y., Gao, J., Huang, R.-J., Liu, S., Huang, Y., Zhu, C., Xu, H., Zheng, C., Liu, P., and Xue, Z.: Chemical profiles of urban fugitive dust PM_{2.5} samples in Northern Chinese cities, *Sci. Total Environ.*, 569-570, 619-626, [doi:10.1016/j.scitotenv.2016.06.156](https://doi.org/10.1016/j.scitotenv.2016.06.156), 2016.
- Shi, G., Xu, J., Peng, X., Xiao, Z., Chen, K., Tian, Y., Guan, X., Feng, Y., Yu, H., Nenes, A., and Russell, A. G.: pH of Aerosols in a Polluted Atmosphere: Source Contributions to Highly Acidic Aerosol, *Environ. Sci. Technol.*, 51, 4289-4296, [doi:10.1021/acs.est.6b05736](https://doi.org/10.1021/acs.est.6b05736), 2017.
- i40 Song, S., Gao, M., Xu, W., Shao, J., Shi, G., Wang, S., Wang, Y., Sun, Y., and McElroy, M. B.: Fine-particle pH for Beijing winter haze as inferred from different thermodynamic equilibrium models, *Atmos. Chem. Phys.*, 18, 7423-7438, [doi:10.5194/acp-18-7423-2018](https://doi.org/10.5194/acp-18-7423-2018), 2018a.
- Song, S., Gao, M., Xu, W., Sun, Y., Worsnop, D. R., Jayne, J. T., Zhang, Y., Zhu, L., Li, M., Zhou, Z., Cheng, C., Lv, Y., Wang, Y., Peng, W., Xu, X., Lin, N., Wang, Y., Wang, S., Munger, J. W., Jacob, D., and McElroy, M. B.: Possible heterogeneous hydroxymethanesulfonate (HMS) chemistry in northern China winter haze and implications for rapid sulfate formation, *Atmos. Chem. Phys. Discuss.*, <https://doi.org/10.5194/acp-2018-1015>, in review, 2018b.
- i45 Sun, Y., Wang, Z., Fu, P., Jiang, Q., Yang, T., Li, J., and Ge, X.: The impact of relative humidity on aerosol composition and evolution processes during wintertime in Beijing, China, *Atmos. Environ.*, 77, 927-934, [doi:10.1016/j.atmosenv.2013.06.019](https://doi.org/10.1016/j.atmosenv.2013.06.019), 2013.
- i50 Sun, Y., Jiang, Q., Wang, Z., Fu, P., Li, J., Yang, T., and Yin, Y.: Investigation of the sources and evolution processes of severe haze pollution in Beijing in January 2013, *J. Geophys. Res. -Atmos.*, 119, 4380-4398, [doi:10.1002/2014jd021641](https://doi.org/10.1002/2014jd021641), 2014.
- Sun, Y., Du, W., Fu, P., Wang, Q., Li, J., Ge, X., Zhang, Q., Zhu, C., Ren, L., Xu, W., Zhao, J., Han, T., Worsnop, D. R., and Wang, Z.: Primary and secondary aerosols in Beijing in winter: sources, variations and processes, *Atmos. Chem. Phys.*, 16, 8309-8329, [doi:10.5194/acp-16-8309-2016](https://doi.org/10.5194/acp-16-8309-2016), 2016.
- i55 Tan, Z., Lu, K., Jiang, M., Su, R., Dong, H., Zeng, L., Xie, S., Tan, Q., and Zhang, Y.: Exploring ozone pollution in Chengdu, southwestern China: A case study from radical chemistry to O₃-VOC-NO_x sensitivity, *Sci. Total Environ.*, 636, 775-786, [doi:10.1016/j.scitotenv.2018.04.286](https://doi.org/10.1016/j.scitotenv.2018.04.286), 2018.
- i60 Ullerstam, M., Johnson, M. S., Vogt, R., and Ljungström, E.: DRIFTS and Knudsen cell study of the heterogeneous reactivity of SO₂ and NO₂ on mineral dust, *Atmos. Chem. Phys.*, 3, 2043-2051, [doi:10.5194/acp-3-2043-2003](https://doi.org/10.5194/acp-3-2043-2003), 2003.
- Usher, C. R., Michel, A. E., and Grassian, V. H.: Reactions on Mineral Dust, *Chem. Rev.*, 103, 4883-4940, [doi:10.1021/cr020657y](https://doi.org/10.1021/cr020657y), 2003.
- i65 Wang, G., Zhang, R., Gomez, M. E., Yang, L., Levy Zamora, M., Hu, M., Lin, Y., Peng, J., Guo, S., Meng, J., Li, J., Cheng, C., Hu, T., Ren, Y., Wang, Y., Gao, J., Cao, J., An, Z., Zhou, W., Li, G., Wang, J., Tian, P., Marrero-Ortiz, W., Secret, J., Du, Z., Zheng, J., Shang, D., Zeng, L., Shao, M., Wang, W., Huang, Y., Wang, Y., Zhu, Y., Li, Y., Hu, J., Pan, B., Cai, L., Cheng, Y., Ji, Y., Zhang, F., Rosenfeld, D., Liss, P. S., Duce, R. A., Kolb, C. E., and Molina, M. J.: Persistent sulfate formation from London Fog to Chinese haze, *Proc. Natl. Acad. Sci.*, 113, 13630-13635,



doi:10.1073/pnas.1616540113, 2016.

- 70 Wang, G., Zhang, F., Peng, J., Duan, L., Ji, Y., Marrero-Ortiz, W., Wang, J., Li, J., Wu, C., Cao, C., Wang, Y., Zheng, J.,
Secretst, J., Li, Y., Wang, Y., Li, H., Li, N., and Zhang, R.: Particle acidity and sulfate production during severe haze
events in China cannot be reliably inferred by assuming a mixture of inorganic salts, *Atmos. Chem. Phys.*, 18,
10123-10132, doi:10.5194/acp-18-10123-2018, 2018a.
- 75 Wang, G., Zhang, F., Peng, J., Duan, L., Ji, Y., Marrero-Ortiz, W., Wang, J., Li, J., Wu, C., Cao, C., Wang, Y., Zheng, J.,
Secretst, J., Li, Y., Wang, Y., Li, H., Li, N., and Zhang, R.: Particle acidity and sulfate production during severe haze
events in China cannot be reliably inferred by assuming a mixture of inorganic salts, *Atmos. Chem. Phys. Discuss.*,
1-23, doi:10.5194/acp-2018-185, 2018b.
- 80 Wang, Y., Zhang, Q. Q., He, K., Zhang, Q., and Chai, L.: Sulfate-nitrate-ammonium aerosols over China: response to
2000–2015 emission changes of sulfur dioxide, nitrogen oxides, and ammonia, *Atmos. Chem. Phys.*, 13, 2635-2652,
doi:10.5194/acp-13-2635-2013, 2013.
- 85 Wang, Y., Zhang, Q., Jiang, J., Zhou, W., Wang, B., He, K., Duan, F., Zhang, Q., Philip, S., and Xie, Y.: Enhanced sulfate
formation during China's severe winter haze episode in January 2013 missing from current models, *J. Geophys.
Res.-Atmos.*, 119, 425-440, doi:10.1002/2013jd021426, 2014.
- 90 Wang, Y. X., McElroy, M. B., Jacob, D. J., and Yantosca, R. M.: A nested grid formulation for chemical transport over Asia:
Applications to CO, *J. Geophys. Res. -Atmos.*, 109, D22307, doi:10.1029/2004jd005237, 2004.
- 95 Ying, Q., Wu, L., and Zhang, H.: Local and inter-regional contributions to PM_{2.5} nitrate and sulfate in China, *Atmos.
Environ.*, 94, 582-592, doi:10.1016/j.atmosenv.2014.05.078, 2014.
- Zhang, L.: A size-segregated particle dry deposition scheme for an atmospheric aerosol module, *Atmos. Environ.*, 35,
549-560, doi:10.1016/s1352-2310(00)00326-5, 2001.
- 100 Zhang, L., Liu, L., Zhao, Y., Gong, S., Zhang, X., Henze, D. K., Capps, S. L., Fu, T.-M., Zhang, Q., and Wang, Y.: Source
attribution of particulate matter pollution over North China with the adjoint method, *Environ. Res. Lett.*, 10, 084011,
doi:10.1088/1748-9326/10/8/084011, 2015.
- Zhang, L., Shao, J., Lu, X., Zhao, Y., Hu, Y., Henze, D. K., Liao, H., Gong, S., and Zhang, Q.: Sources and Processes
Affecting Fine Particulate Matter Pollution over North China: An Adjoint Analysis of the Beijing APEC Period,
105 *Environ. Sci. Technol.*, 50, 8731-8740, doi:10.1021/acs.est.6b03010, 2016.
- Zhang, L., Chen, Y., Zhao, Y., Henze, D. K., Zhu, L., Song, Y., Paulot, F., Liu, X., Pan, Y., Lin, Y., and Huang, B.:
Agricultural ammonia emissions in China: reconciling bottom-up and top-down estimates, *Atmos. Chem. Phys.*, 18,
339-355, doi:10.5194/acp-18-339-2018, 2018.
- Zhang, Q., Streets, D. G., Carmichael, G. R., He, K. B., Huo, H., Kannari, A., Klimont, Z., Park, I. S., Reddy, S., Fu, J. S.,
100 Chen, D., Duan, L., Lei, Y., Wang, L. T., and Yao, Z. L.: Asian emissions in 2006 for the NASA INTEX-B mission,
Atmos. Chem. Phys., 9, 5131-5153, doi:10.5194/acp-9-5131-2009, 2009.
- Zhang, R., Jing, J., Tao, J., Hsu, S. C., Wang, G., Cao, J., Lee, C. S. L., Zhu, L., Chen, Z., Zhao, Y., and Shen, Z.: Chemical
characterization and source apportionment of PM_{2.5} in Beijing: seasonal perspective, *Atmos. Chem. Phys.*, 13,
7053-7074, doi:10.5194/acp-13-7053-2013, 2013.



- '05 Zhao, D., Song, X., Zhu, T., Zhang, Z., Liu, Y., and Shang, J.: Multiphase oxidation of SO₂ by NO₂ on CaCO₃ particles, Atmos. Chem. Phys., 18, 2481-2493, doi:10.5194/acp-18-2481-2018, 2018.
- Zheng, B., Zhang, Q., Zhang, Y., He, K. B., Wang, K., Zheng, G. J., Duan, F. K., Ma, Y. L., and Kimoto, T.: Heterogeneous chemistry: a mechanism missing in current models to explain secondary inorganic aerosol formation during the January 2013 haze episode in North China, Atmos. Chem. Phys., 15, 2031-2049, doi:10.5194/acp-15-2031-2015, 2015.
- '10 Zheng, B., Tong, D., Li, M., Liu, F., Hong, C., Geng, G., Li, H., Li, X., Peng, L., Qi, J., Yan, L., Zhang, Y., Zhao, H., Zheng, Y., He, K., and Zhang, Q.: Trends in China's anthropogenic emissions since 2010 as the consequence of clean air actions, Atmos. Chem. Phys., 18, 14095-14111, doi:10.5194/acp-18-14095-2018, 2018.

'15

'20



Tables and Figures

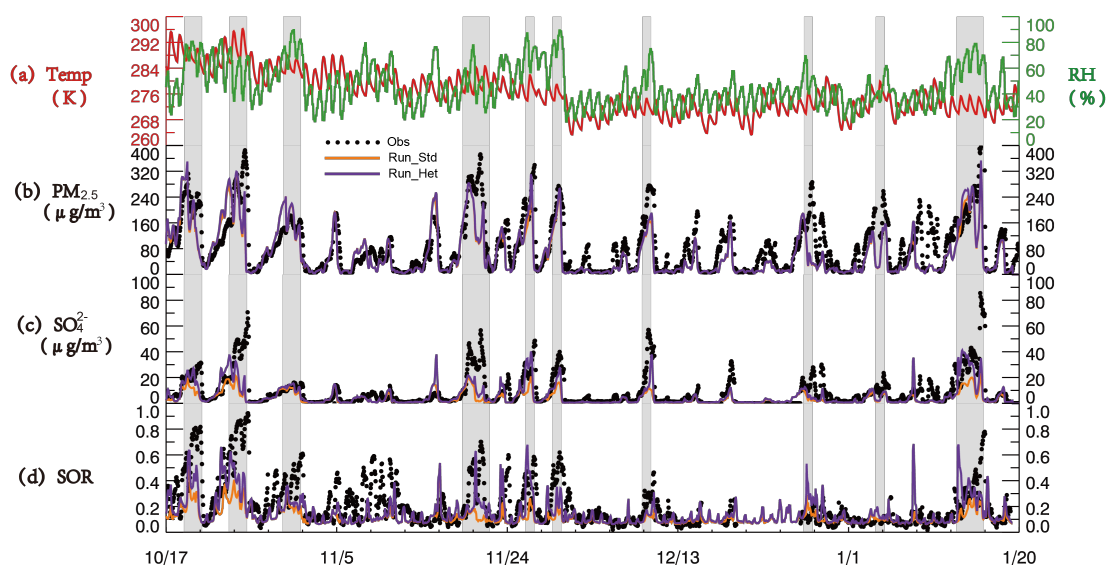
25 **Table 1.** Description of model simulations.

Model run	TMI-catalysis in clouds	Heterogeneous reactions	Aerosol pH	Horizontal resolution
Run_STD	N	N	ISO ^[1]	1/4°×5/16° & 4°×5°
Run_TMI	Y	N	ISO	1/4°×5/16° & 4°×5°
Run_Het	Y	Y	ISO	1/4°×5/16° & 4°×5°
Sensitivity simulations based on Run_Het ^[2]				
Run_pH2	Y	Y	2	4°×5°
Run_pH3	Y	Y	3	4°×5°
Run_pH4	Y	Y	4	4°×5°
Run_pH5	Y	Y	5	4°×5°
Run_pH6	Y	Y	6	4°×5°
Run_pH7	Y	Y	7	4°×5°
Run_pH8	Y	Y	8	4°×5°

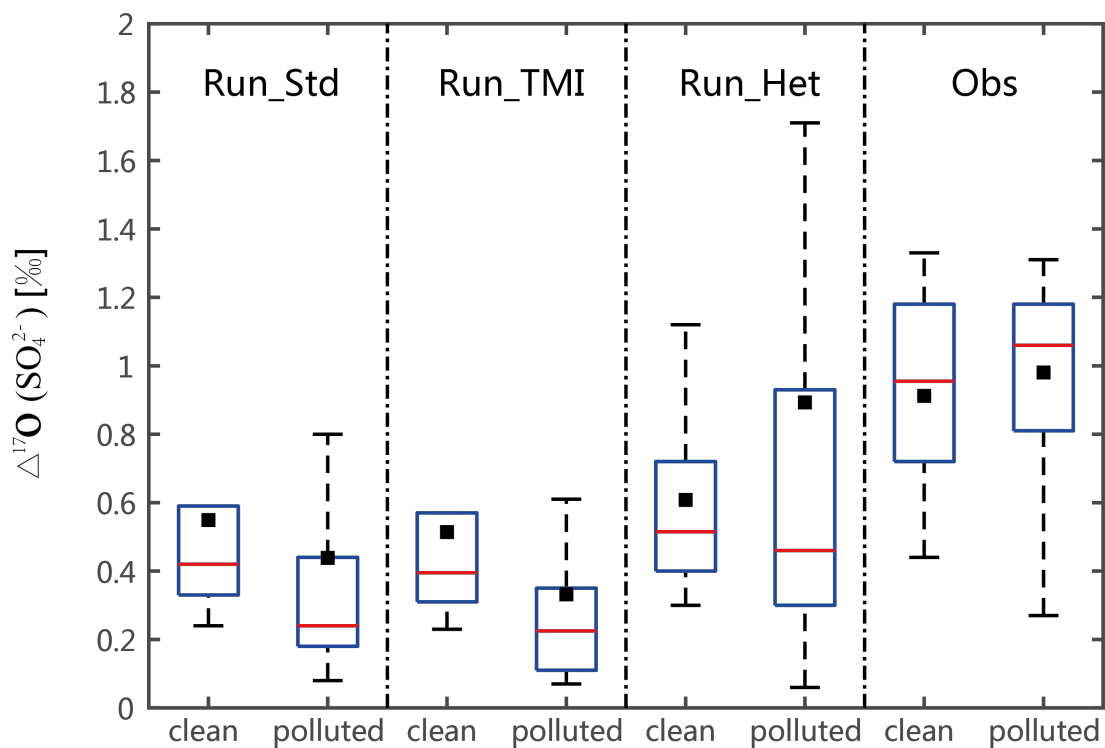
^[1] ISO means that the aerosol pH was calculated by ISORROPIA II in the model assuming metastable state.

^[2] For the sensitivity simulations, aerosol pH was fixed to the stated prescribed value.

30



35 **Figure 1.** Time series of (a) GEOS-FP temperature (red line) and relative humidity (RH; green line), (b) $PM_{2.5}$ and (c) sulfate concentration, and (d) SOR at the surface in Beijing during the study period of 17 October 2014 – 20 January 2015. Hourly $PM_{2.5}$, sulfate, and SOR observations (black dots) are compared with model results from Run_Std (orange line) and Run_Het (purple line). The gray shaded bars represent 10 heavy pollution periods (HPP) ($PM_{2.5} > 150 \mu g m^{-3}$) as defined in the text.



'40

Figure 2. The box charts show observed vs. modeled $\Delta^{17}\text{O}(\text{SO}_4^{2-})$ in Beijing for each model simulation separated for heavy pollution and clean periods. The box line from bottom to top is respectively percentile of 25%, 50% and 75%, the whisker from bottom to top is respectively the minimum and the maximum, and the black square is mean value.

'45

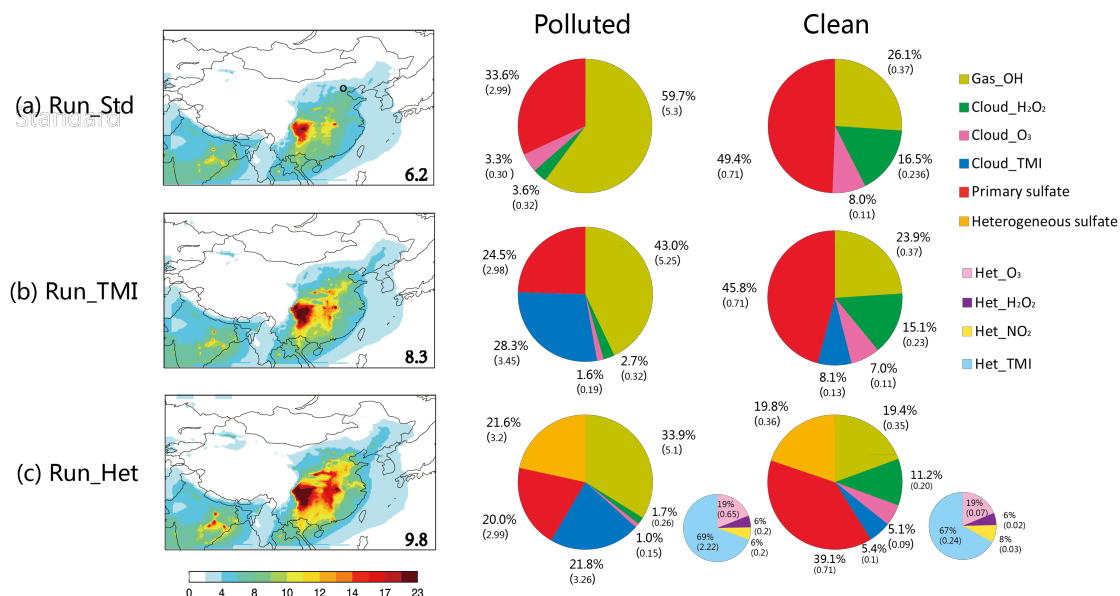


Figure 3. Model simulated sulfate aerosol concentrations ($\mu\text{g m}^{-3}$) above the ground for (a) Run_Std, (b) Run_TMI, and (c) Run_Het. Panels on the left show the spatial distributions with the numbers in inset representing simulated mean sulfate concentrations in Beijing (black circle in (a)) during the entire measurement period. The middle and right columns show percent contributions of different sulfate formation pathways to sulfate aerosol concentration in Beijing as calculated by the different model runs during polluted (HPP) and clean (CP) periods, respectively. The smaller pie charts in (c) show relative contributions of the four heterogeneous sulfate formation pathways implemented in the model. Numbers are percentage contributions (%) and absolute sulfate concentration ($\mu\text{g m}^{-3}$) are in parentheses.

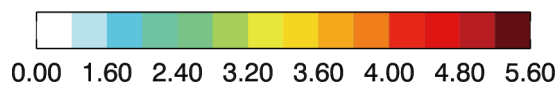
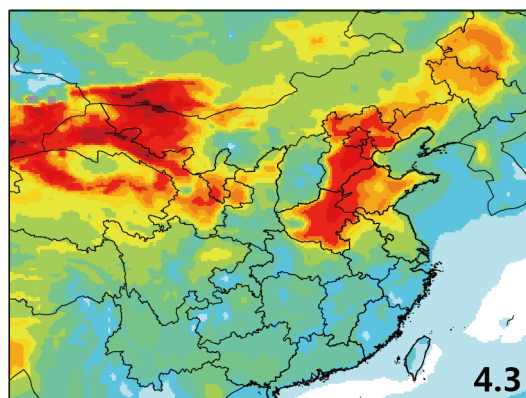
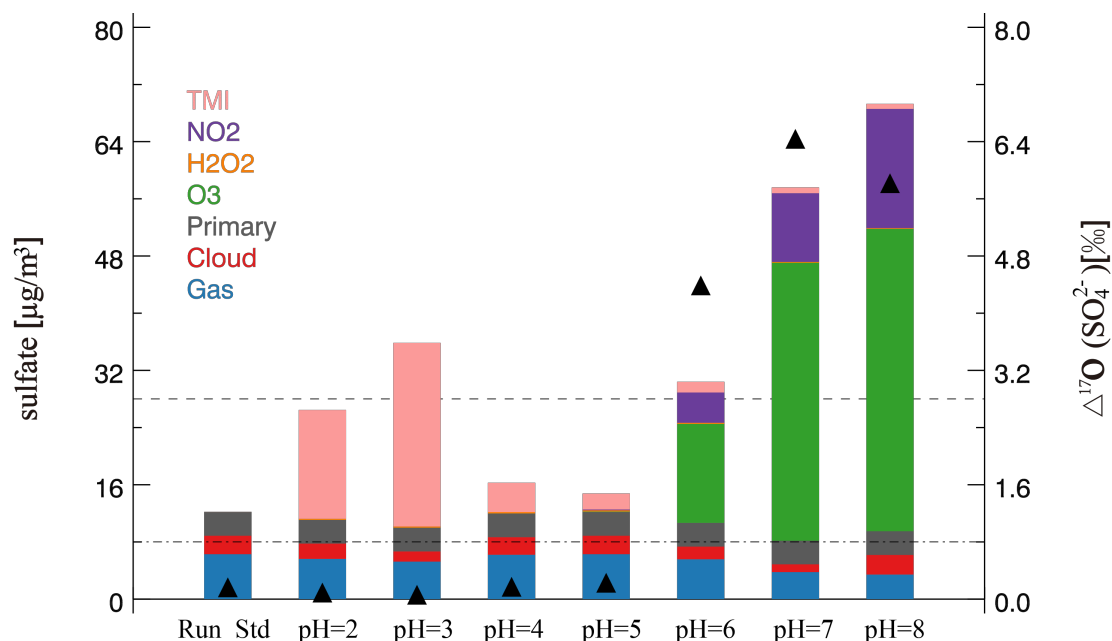


Figure 4. Model simulated mean aerosol pH values at the surface of China from 17 October 2014 to 20 January 2015 from Run_Het. Number in inset represents mean calculated pH values in Beijing.

'60



'65

'70

Figure 5. Model simulated mean sulfate concentration in Beijing averaged over heavy pollution periods (HPP as defined in the text). Model results are from the standard simulation (Run_Std) and sensitivity simulations with prescribed aerosol pH ranging 2 to 8. Different colors represent contributions from different sulfate formation pathways, including four heterogeneous reactions (oxidation by O₂ (TMI), NO₂, H₂O₂, O₃), primary anthropogenic, aqueous-phase oxidation in clouds, and gas-phase oxidation. Also shown are the corresponding modeled Δ¹⁷O(SO₄²⁻) values in Beijing (black triangles). The dashed line denotes observed mean sulfate concentration (25.9 μg m⁻³), and the dot-dashed line denotes observed mean Δ¹⁷O(SO₄²⁻) (0.9‰) during HPP in Beijing.